J. Phys.: Condens. Matter **11** (1999) 2707–2717. Printed in the UK PII: S0953-8984(99)98586-7

Domain wall pinning at an interface step defect

A L Dantas† and A S Carriço‡§

† Faculdade de Ciências Naturais, Universidade Estadual do Rio Grande do Norte, Mossoró, RN 59610-210, Brazil

‡ Departamento de Física, Universidade Federal do Rio Grande do Norte, Natal, RN 59072-970, Brazil

Received 20 October 1998, in final form 26 January 1999

Abstract. We study the magnetization of a thin uniaxial ferromagnetic film on a two-sublattice uniaxial antiferromagnetic substrate near an interface step defect. The step defect produces two distinct regions where opposite sublattices of the antiferromagnet adjoin the interface. We show that the proximity interaction with the substrate leads to the formation and pinning of a Néel domain wall centred at the step edge. The equilibrium pattern is obtained using a numerical procedure which allows for rearrangement of the magnetization of the ferromagnet, which adjusts itself under the effect of the interface field. Our results indicate that the wall profile is rather close to a free-wall pattern; however, the proximity interaction may lead to considerable reduction of the domain wall width. We find that the interface coupling controls the magnetization for weak fields applied along the easy axis. In this case the magnetization results from rigid displacement of the wall, favouring the growth of the domain magnetized in the field direction. The wall detaches from the defect, and the magnetization saturates, when the applied-field strength reaches the value of the interface exchange field associated with the proximity interaction. For a weak external field applied perpendicular to the step edge direction, the magnetization is due to the orientation of the domains in the field direction. In this case saturation occurs for much larger applied-field strength.

1. Introduction

The effect of the substrate on the magnetic properties of thin ferromagnetic films is a subject of continuing interest. A number of relevant magnetic features are related to the influence of the interface on the equilibrium state of the ferromagnet [1].

The stabilization of large domains in thin ferromagnetic films on antiferromagnetic substrates is an issue of current technological interest [2]. The effectiveness of the antiferromagnetic substrate in this context relies upon the large values of the anisotropy, found in antiferromagnets (AF) of current interest, as compared to the typical values of the ferromagnetic anisotropy-field strength. Since the antiferromagnet is more stable against field effects, it may hold the ferromagnet (F) in a single-domain state even at external-field strengths that would normally reverse the magnetization of the ferromagnet.

The proximity effect, which describes the interaction between the ferromagnetic film and the antiferromagnetic substrate, was proposed in a different scenario many years ago [3]. It was found that oxidation of Co samples leads to remarkable modifications of the hysteresis curve. The observed hysteresis shifts and coercivity changes were attributed to an interface

§ Author to whom any correspondence should be addressed. E-mail address: acarrico@dfte.ufrn.br; fax: (55)(84)2153791.

0953-8984/99/132707+11$19.50

bias field that results from the formation of antiferromagnetic CoO layers surrounding the Co microcrystals of the sample.

Interface roughness impacts in a relevant manner on the effectiveness of the interface bias field. The interface exchange energy is proportional to the net magnetization of the antiferromagnet at the interface. For a uniaxial two-sublattice antiferromagnetic substrate, one may find either sublattice at the interface. The overall effect of the F/AF interaction depends on the relative values for the areas where each AF sublattice adjoins the interface. Magnetization measurements involve macroscopic areas of the interface. Therefore the hysteresis curves do not reveal the local contact interaction. Instead they provide information about a macroscopic average of the effective interface exchange field.

The formation of domain walls in response to spatial variations in the sign of the effective interface coupling, associated as they may be with the interface roughness, is subject to certain general conditions. If the density of interface defects is too high, there is no room for complete rotation of the magnetization of the ferromagnet. In this case the ferromagnet can hardly be affected by interface defects. If the defect density is small, then each defect will act independently as a possible domain wall nucleation centre. The width of the ferromagnet domain wall is a parameter which might be useful to guide this discussion. If the average distance between defects is much larger than the domain wall width, then the intrinsic domain wall nucleation strength of each defect will show up in full. In this case the discussion of domain wall nucleation can be restricted to a single-defect problem.

Interface defect pinning may lead to considerable reduction of the domain wall width. Therefore the intrinsic domain wall width of the ferromagnetic film is not a good parameter for the description of interface effects. Judging from the intrinsic value of the domain wall width, one might expect that low-anisotropy materials would not be affected by a large density of interface defects. These materials have wide domain walls; thus one might think that the uniform magnetization state would be stable, if the interface roughness is large, although the ferromagnetic film is subjected to strong exchange coupling to the antiferromagnetic substrate. On the other hand, low-anisotropy materials are expected to be the most affected by the interface effective exchange field. In these materials the domain wall energy is small and the interface exchange energy may control the magnetization profile, if the interface exchange field is of the order of the intrinsic ferromagnetic exchange field [4].

The field of domain walls is in many respects equivalent to the field of soliton-like systems [5]. Interesting results on the stability of kink solitons in the presence of external forces [6] have been reported recently.

In the present work we study the nucleation of domain walls centred at a step defect on the interface between a ferromagnetic thin film and an antiferromagnetic substrate. The

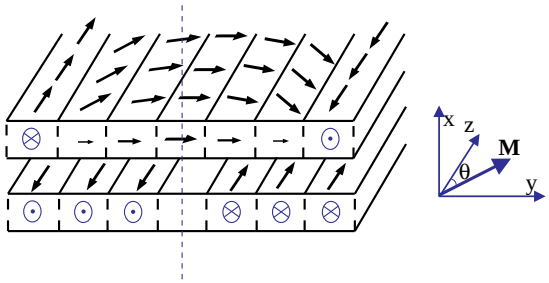

Figure 1. A sketch of a Néel wall pinned at a step defect on an antiferromagnetic substrate.

model consists of a thin uniaxial ferromagnetic film with in-plane magnetization, on a two-sublattice uniaxial antiferromagnet substrate, as seen in figure 1. The anisotropy axis of the antiferromagnet is parallel to the easy direction of the ferromagnet (the z-axis). The substrate step edge runs along the z-axis and divides the substrate into two regions, each one containing spins from a sublattice of the antiferromagnet. The effective interface exchange field has a discontinuous change of direction at the step edge. In our model no accommodation is made for the substrate, which is considered frozen in the antiferromagnetic state.

In section 2 we describe the numerical method used to obtain the equilibrium magnetization pattern of the ferromagnet. In section 3 we discuss the modification of the wall profile of the ferromagnet produced by the interface defect. In section 4 we study field effects, and the final section is devoted to the discussion of the results and applications for systems of current interest.

2. Equilibrium configuration

The substrate effect is represented by a contact exchange interaction energy J_{int}, which is a minimum when the ferromagnetic moments are in the opposite direction to the moments of the antiferromagnetic substrate at the interface. While the intrinsic exchange and anisotropy energies of the ferromagnet create an energy barrier to wall nucleation, the substrate step defect tends to nucleate a π-wall in the ferromagnet. Wall nucleation occurs if the interface coupling energy is sufficiently strong to overcome the intrinsic barrier.

No magnetization variation along the z-axis direction is allowed. Also, as appropriate for thin films, we do not consider any variation of magnetization along the x-axis direction. Therefore the magnetic energy, per unit wall area, is given by

$$E = \sum_n \left(-J_0 \vec{S}_n \cdot \vec{S}_{n+1} - J_{int} S_{nz} - \frac{K}{2} S_{nz}^2 - g\mu_B \vec{S}_n \cdot \vec{H} \right) \tag{1}$$

where J_0 and J_{int} are the intrinsic and interface exchange constants, K is the uniaxial anisotropy constant, $\vec{H}$ is the applied field, and S_{nz} is the z-component of $\vec{S}_n$. The actual change of direction of the substrate moments is represented by a change of the sign of J_{int}, which is given by

$$J_{int} = \begin{cases} J & \text{for } n < 0 \\ -J & \text{for } n > 0. \end{cases} \tag{2}$$

This kind of interface exchange coupling leads to the domain configuration shown in figure 1.

The effectiveness of the interface exchange coupling for domain wall nucleation depends on the relative values of the domain width, ω, and the domain wall width. We study here the case of large domains. Notice that while the intrinsic energy barrier, $4(AK)^{1/2}$, is independent of the domain width [7], the interface coupling energy is a strongly decreasing function of the ω. Apart from the contribution of the domain wall region, the interface exchange energy is roughly of the order of $-2\omega J$. Thus for wide domains the threshold value of J for domain wall nucleation is negligible.

Throughout the text we make reference to the interface effect either by using the value of the effective interface exchange coupling energy (J) or the associated effective field $H_J = J/g\mu_B$. Furthermore, we will also use the exchange stiffness of the ferromagnet, A, which is proportional to J_0, and the anisotropy field of the ferromagnet, $H_a = KS/g\mu_B$, where S is the thermal saturation value of the ferromagnetic spins.

The magnetic structure is represented by spins, with y- and z-axis components, along a linear chain. As appropriate to most systems of current interest, no temperature effects

are considered, and the spins have the saturation value S. Therefore, in order to describe the magnetic structure, we calculate the angles that each spin makes with the z-axis, $\{\theta_n, n = 1, \ldots, N\}$. The equilibrium pattern is found by requiring that each magnetic moment along the chain be parallel to the local effective field [8]. We use a self-consistent algorithm to find the equilibrium profile. Here we just give a brief outline of the method and the reader is referred to reference [8] for further details.

The effective field acting on each spin is obtained from the gradient of the energy, with respect to the spin components. After initializing all the spin variables $\{\theta_n, n = 1, \ldots, N\}$, the effective field is calculated at each site of the chain. If parallelism is found between the local field and the spins at all sites, within a given precision (typically 10^{-7}), then the equilibrium condition is satisfied. Otherwise, the effective-field profile in the chain is used to reinitialize the spin variables.

The process is repeated until the equilibrium condition is satisfied. The number of spins in the chain, N, is chosen such that no artificial end effects are introduced in the results. N is chosen much larger than the number of spins within a domain wall width. Therefore for low values of the anisotropy constant K, large chains are used. In any case we check that the results are independent of N. We generally find that the convergence is more difficult to achieve for low values of the anisotropy and interface exchange coupling, and also when the Zeeman energy is comparable to the interface energy. In these cases a large number of iterations are required to obtain the equilibrium pattern. A final check is made to ensure that the energy of the π-wall state is lower than the energy of the uniform state.

3. Magnetization profiles

With the external field set to zero, we analyse the effects of the interface exchange coupling in the magnetization profile near the defect. We have found that if $\omega \gg \Delta_0$ then a domain wall is stabilized by the defect even though the value of the interface exchange coupling J is quite small. In this section we discuss the effect of the interface exchange on the domain wall profile. In the figures we give the effective interface field, the external field, and the anisotropy field in units of the intrinsic exchange field of the ferromagnet ($H_e = 2J_0S/g\mu_B$).

The values of the interface exchange coupling and the anisotropy of the ferromagnet are key parameters for our discussion. The interface coupling favours the formation of narrow domain walls. In the domain wall region the spins are nearly perpendicular to the interface field. As the width of the domain wall region is reduced, the areas of the ferromagnetic domains, on each side of the defect edge, increase. Since in the domains the spins of the ferromagnet are aligned with the interface field, we find that reducing the domain wall width contributes to the enhancing of the interface effect and the stabilizing of the domain wall.

It is instructive to discuss the domain wall profiles with reference to the intrinsic pattern of the ferromagnetic Néel wall. In a free wall the angle that the magnetization density makes with the easy axis is given by

$$\tan\frac{\theta}{2} = \exp\left(\frac{y}{\Delta_0}\right) \tag{3}$$

where $\pi\Delta_0 = \pi(A/K)^{1/2}$ is the domain wall width. We use this result below to study the shape of a domain wall pinned at an interface defect.

Our results show that the effect of the proximity interaction, even for relatively large values of the interface effective exchange field, is to modify the domain wall width; however, the free-wall profile is maintained. We have found that equation (3) applies to the magnetization pattern of a Néel wall pinned at the interface defect, provided that the domain wall parameter, Δ_0, is

substituted for with a J-dependent domain wall parameter, Δ, which is a decreasing function of the interface exchange coupling strength.

In figure 2 we show $\ln(\tan(\theta_n/2))$ as a function of the position near the domain wall centre for a ferromagnetic film with $H_a/H_e = 0.05$. It is readily seen that the profile is rather similar to the free-wall pattern, except for the reduction of the domain wall width. The slopes of the curves increase with increasing J, indicating that the width of the domain wall decreases as J is increased. For the chosen values of H_J/H_e the magnetization pattern is given by equation (3) with the domain wall width reduced by the coupling to the substrate. Notice that, even though for $H_J/H_e = 0.3$ the interface field is much larger than the anisotropy field, the free-wall profile is maintained, with a modified domain wall width. We have found that for stronger values of J (results not shown) the free-wall profile is not valid. In this limit there are strong modifications of the magnetic profile near the wall centre.

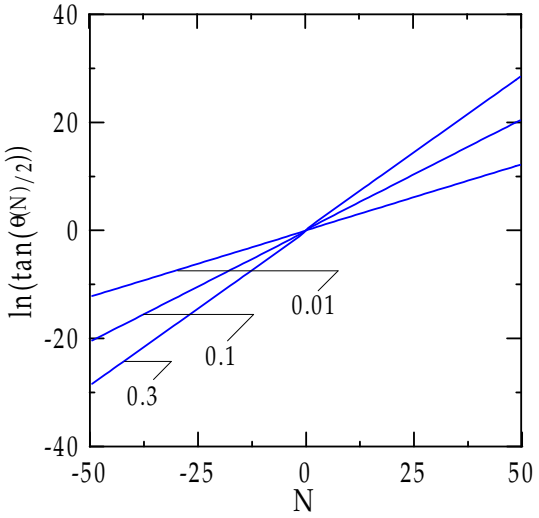

Figure 2. $\ln(\tan(\theta/2))$ is shown for comparison with the intrinsic wall profile. Only the domain wall region is shown. The numbers by the curves indicate the values of H_J/H_e. The interface field is scaled by the intrinsic exchange field.

In order to examine the role of the anisotropy we calculated the domain wall width as a function of the interface exchange coupling, for selected values of H_a/H_e. The effect of the interface coupling is to reduce the domain wall width, since this leads to larger areas of the interface complying with the trend imposed by the discontinuous change in the interface exchange energy. Large values of the anisotropy impose a limit on the interface effect, since the cost of reducing the domain wall width becomes larger.

The domain wall width is given by $\pi/|\partial\theta/\partial y|_{y=0}$. For a free-wall profile, as in equation (3), the domain wall width is equal to $\pi\Delta$. We obtain the domain wall width from the inverse of the difference of the angles near the wall centre. In figure 3 we show Δ/Δ_0, where Δ_0 is obtained from the numerical calculation for a fairly small value of J ($H_J = 10^{-3}H_e$). We have found that the reduction of the domain wall width is stronger for low anisotropy values, as expected. For high values of J there are relevant modifications of the profile, compared to the intrinsic form of equation (3).

These results indicate that strong reductions of the domain wall width are expected in interfaces of current interest. In figure 3 we see that the reduction in Δ is stronger for low anisotropy values. The curve for $H_a/H_e = 0.05$ decreases more rapidly with J than the others.

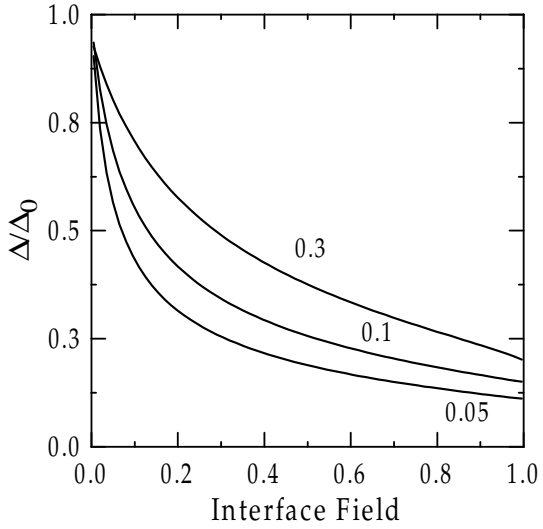

Figure 3. The domain wall width as a function of the interface exchange coupling. The numbers by the curves indicate the values of H_a/H_e.

Furthermore, for all chosen values of the anisotropy, the reduction in domain wall width is larger than 50% for $H_J/H_e = 0.3$. Notice that for $H_a/H_e = 0.05$ the maximum reduction in the domain wall width is around 85%. This might be of interest for the study of the effect of interface roughness in low-anisotropy materials, as discussed below.

4. Field effects

In figure 4 we display the magnetization curves for an external field applied in the z-axis direction and four values of the strength of the interface exchange field. For small values of the applied-field strength, the magnetization is proportional to the applied field. Saturation occurs when the applied-field value equals the interface exchange field. At this field the wall detaches from the step defect and the whole film aligns with the applied field. In the figure we display the magnetization values over a limited applied-field interval. The magnetization is rather small for weak fields and rises rapidly to saturation for applied-field values near the interface exchange field. In order to display the differences in $M(H)$ for a few values of the interface exchange field (J) we show only a fraction of the calculated curves prior to saturation.

For small applied-field values, $H \ll H_e$, the linear relation of the magnetization and field is due to rigid domain wall displacement. The displacement of the wall centre from the step defect is proportional H and no appreciable distortion is found relative to the profile corresponding to $H = 0$. Therefore the magnetization increases as a result of domain growth. We have found that for larger values of H the domain wall displacement is not proportional to the applied-field strength. Also, for large values of H, appreciable distortions of the wall profile are produced and then the magnetization is no longer proportional to the applied field.

We have also calculated the domain wall width as a function of the applied field, by examining the inverse gradient of the angle with the easy axis near the domain wall centre. Although these results are not shown here, it is instructive to note that the domain wall width does not change for low values of H, confirming that at low field values the magnetization is due to rigid displacement of the wall.

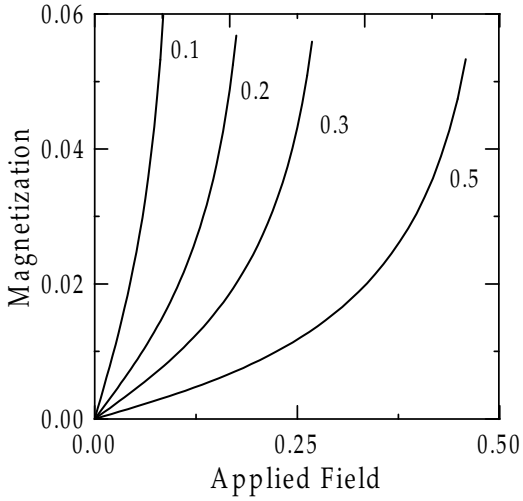

Figure 4. Magnetization curves for an external field applied along the easy axis. The magnetic field is shown in units of the intrinsic exchange field H_e. The numbers by the curves indicate the values of H_a/H_e.

Also notice from figure 4 that for low values of the external field strength the static susceptibility is larger if the interface coupling is weak. This is the expected behaviour since only rigid displacement occurs for small values of H. No intrinsic exchange energy or anisotropy energy is involved in the rigid wall displacement. Instead, the equilibrium position of the wall centre, for a given value of the applied-field strength, is determined by the balance between the interface exchange energy and the Zeeman energy. Therefore larger displacements of the domain wall centre are required to balance the Zeeman energy if the interface coupling is weak (small J-values).

In figure 5 we display the $\theta(y)$ profiles for $H_J/H_e = 0.005$ and $H_a/H_e = 0.05$, and for $H = 0$ and $H/H_J = 0.6$ and $H/H_J = 0.9$. We have selected the region around the domain wall centre, so that a clear comparison between the three profiles can be made visually. The position is scaled with respect to the domain wall width, and the region shown corresponds to the width of two domain walls. For the chosen value of H_J/H_e the domain wall width is practically equal to the intrinsic value ($\Delta = \Delta_0$). The maximum value chosen for the applied field ($H/H_J = 0.9$) is close to the saturation value; even so, there is no noticeable modification of the wall profile. The curve for $H/H_J = 0.6$ is clearly the $H = 0$ curve displaced rigidly. Also notice that on increasing the applied field by 50%, from $H/H_J = 0.6$ to $H/H_J = 0.9$, the displacement practically doubles. The linear dependence of the domain wall displacement on the applied field is valid only for small values of H.

In the inset in figure 5 we show the value of the angle θ at the step discontinuity. For $H = 0$ the domain wall is centred at the step edge ($y = 0$); thus $\theta(0) = \pi/2$. The field displaces the domain wall to the right, favouring the growth of the $\theta = 0$ domain. Thus the value of $\theta(0)$ decreases as H increases. From the figure it is clear that $\theta(0)$ decreases linearly with H for small values of H. The linear dependence of $\theta(0)$ on H can be understood on the basis of a simple argument. Assuming a rigid wall displacement, induced by the applied field, we have

$$\tan\frac{\theta}{2} = \mathrm{e}^{(y-q)/\Delta}. \tag{4}$$

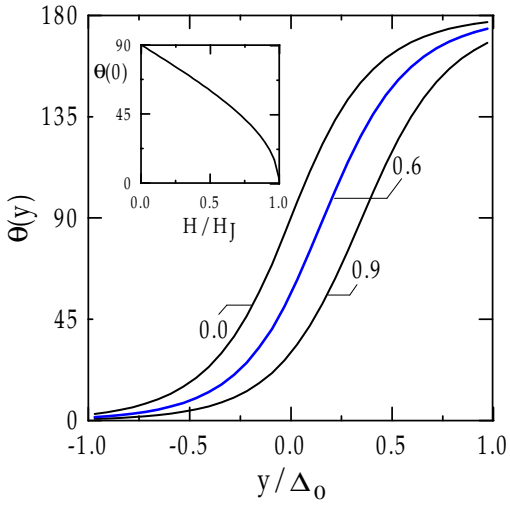

Figure 5. Domain wall profiles showing rigid wall displacement, for $H_a/H_e = 0.05$ and $H_J/H_e = 0.005$. The position is shown in units of the domain wall width and the numbers by the curves indicate the values of the applied field in units of the interface exchange field. In the inset we show the value of the angle at the step defect ($y = 0$) as a function of the applied-field strength. In this picture the applied field is shown in units of the interface exchange field.

Thus if the wall displacement (q) is proportional to H, then at $y = 0$ we have

$$\tan\frac{\theta(0)}{2} = \mathrm{e}^{-\eta H/\Delta} \tag{5}$$

where $q = \eta H$ was used. Expanding the right-hand side of equation (5) for low values of

$$\frac{q}{\Delta} = \frac{-\eta H}{\Delta}$$

we get

$$\theta(0) = \frac{\pi}{2} - \frac{\eta}{\Delta}H \tag{6}$$

as seen in the inset in figure 5.

If the external field is applied along the y-axis the magnetization process involves different stages. In this case the external field is parallel to the magnetization at the domain wall centre. The main field effect, for weak fields, is to rotate the domain magnetization towards the field direction. Since the domain region is much larger than the domain wall region, the magnetic structure is determined by the energy balance in the domains. Thus, we may calculate analytically the orientation of the magnetization in the domains and also the total magnetization. The energy density in the left-hand domain is given by

$$\varepsilon_D = -\frac{K}{2}\cos^2\theta - J\cos\theta - M_s H\sin\theta \tag{7}$$

where θ is the angle made with the z-axis and M_s is the saturation value of the magnetization. For small values of H the domain magnetization is practically aligned with the easy axis ($\theta \simeq 0$); the deviation from parallelism with the interface field is proportional to the value of the applied field. In this limit, minimizing the energy density, given by equation (7), with respect to θ gives

$$\theta = \frac{H}{H_a + H_J}. \tag{8}$$

In the right-hand domain we find that the magnetization also tilts towards the field direction and the angle made with the z-axis is $\pi - \theta$. For high values of H there are field-induced modifications of the domain wall structure and the simple argument ceases to be valid.

The y-component of the magnetic moment per unit wall area is given by

$$\mu_y = \int_{\text{domains}} M_y \, \mathrm{d}y + \int_{\substack{\text{domain}\\ \text{wall}}} M_y \, \mathrm{d}y. \tag{9}$$

The integral over each domain is of the order of the domain width (ω) and the integral over the domain wall is of the order of Δ. Therefore in the limit of $\omega \gg \Delta$ the magnetization is due to the progressive orientation of the domains in the field direction. In reduced units, $m = \mu_y / 2\omega M_s$, we have

$$m = \frac{1}{\omega} \int_{-\omega}^{0} \sin\theta \, \mathrm{d}y = \frac{H}{H_a + H_J}. \tag{10}$$

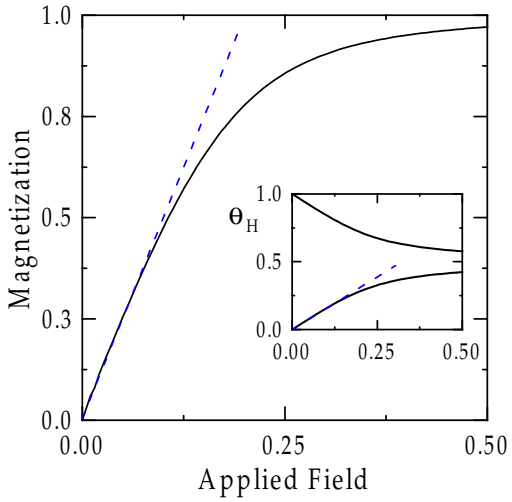

Figure 6. The reduced magnetization for an external field applied perpendicular to the easy axis for $H_a/H_e = 0.1$ and $H_J/H_e = 0.1$. The applied field is shown in units of the intrinsic exchange field. In the inset we show the angles, in units of π radians, between the magnetization, in each of the domains, and the easy axis. Continuous curves display the numerical results and the broken curves show the analytical results obtained from equation (10) and equation (8).

In figure 6 we plot the numerically calculated y-component of the magnetization for a field applied along the y-axis and for $H_a/H_e = H_J/H_e = 0.1$. In the inset in figure 6 we show the calculated values of the domain angles, as functions of the applied-field strength. The dashed curves show the values of the y-component of the magnetization as given by equation (10), and the angle between the magnetizations and the easy axis in the domains, as given by equation (8). It is readily seen that the slopes of both curves agree with the predictions of the numerical calculations for small values of H/H_e. Furthermore, it is clear that the saturation of the magnetization occurs for a value of the applied field much larger than the interface exchange field. It is instructive to compare this figure with figure 4.

5. Conclusions

We have shown that a step defect in an F/AF interface pins a Néel wall whose domain wall width may be severely reduced with respect to the intrinsic value, especially for low-anisotropy

ferromagnets.

The magnetization curves for an external field applied along the step edge and perpendicular to it reveal special features. While in the first case the magnetization, for low field values, is due to domain wall displacement, in the second case it is due to the orientation of the magnetization in the domains in the direction of the applied field. The interface exchange coupling may be obtained from the analysis of the magnetization curves. With the external field applied along the step edge, the magnetization saturates when $H = H_J$. For a field applied perpendicular to the step edge, equation (10) may be used to obtain the value of the interface exchange field. The static perpendicular susceptibility at low field strength is a function of H_J.

Notice that for single-domain uniform rotation, under a perpendicular external field H, the perpendicular susceptibility is $1/H_a$, and the saturation of the magnetization occurs for $H = H_a$ [9]. The small-field perpendicular susceptibility of a Néel wall pinned at an interface defect may be much smaller than $1/H_a$, since H_J is likely to be stronger than the anisotropy field. Furthermore, as seen in figure 6, saturation occurs for an applied-field strength much larger than H_a.

We have chosen values of the anisotropy–exchange-field ratio (H_a/H_e) of the same order of magnitude as those for F/AF Fe/Cr, Co/CoO, NiFe/CoO bilayers [10]. The value of the interface effective field (H_J) is not precisely known. Most experimental techniques sample large areas of the interface, so the data are likely to represent average values of H_J. Thus we have used the value of H_J as a free parameter, in order to examine the trends imposed by the interface effect.

The present results may be helpful in interpreting magnetization measurements made on virgin samples of thin ferromagnetic films on antiferromagnetic substrates. Real interfaces may exhibit areas of reversed AF sublattice against a background of the other sublattice. If the height of these regions, relative to the background substrate level, is an odd number of lattice parameters of the antiferromagnet, then at the borders of these regions there is a change of π in the direction of the interface effective field. Thus each border will act as a domain wall nucleation centre. We have shown that for low-anisotropy materials the reduction of the domain wall width, caused by interface effects, may be quite strong. Therefore the accommodation of the ferromagnet's magnetization to changes in the interface coupling occurs in small areas in the neighbourhood of the borders where the AF sublattice changes. Thus, unless there is appreciable change in the antiferromagnet's easy-axis direction, over the interface, the overall magnetization of virgin F/AF samples, with interface roughness, might display the features discussed here.

Our results may also be helpful for interpreting magnetization measurements made on thin ferromagnetic films on vicinal AF substrates [11], which may exhibit a periodic structure of terraces with opposite sublattices.

Acknowledgments

We thank the Brazilian Research Council CNPq and CAPES for partial financial support.

References

[1] Jonge W J M, Bloemen P J H and Boreger F J A 1994 *Ultrathin Magnetic Structures I* ed B Heinrich and J A C Bland (Berlin: Springer) p 64

[2] Parkin S S P 1996 *Proc. Symp. on Magnetism in Metals (Copenhagen*) ed D F McMorrow, J Jensen and H M Ronnow (Copenhagen: The Royal Danish Academy of Sciences and Letters) p 113

Tsang C and Fontana R 1982 *IEEE Trans. Magn.* **18** 1149

[3] Meiklejohn W H and Bean C P 1957 *Phys. Rev.* **105** 204
[4] Malozemoff A P 1987 *Phys. Rev.* B **35** 3679
Malozemoff A P 1988 *J. Appl. Phys.* **63** 3874
[5] Mikeska H J and Steiner M 1991 *Adv. Phys.* **40** 191
[6] Holyst J A 1998 *Phys. Rev.* B **57** 4786
González J A and Holyst J A 1992 *Phys. Rev.* B **45** 10 338
[7] See for instance Zijlstra H 1987 *Ferromagnetic Materials* vol 3, ed E P Wohlfarth (Amsterdam: North-Holland) ch 2
[8] Camley R E and Tilley D R 1988 *Phys. Rev.* B **37** 3413
Nortemann F C, Stamps R L, Carriço A S and Camley R E 1992 *Phys. Rev.* B **46** 10 847
Carriço A S and Camley R E 1992 *Phys. Rev.* B **45** 13 117
[9] See for instance Morrish A H 1965 *The Physical Principles of Magnetism* (New York: Wiley) ch 7
[10] Fullerton E E, Conover M J, Mattson J E, Sowers C H and Bader S D 1993 *Phys. Rev.* B **48** 15 755
Nogues J, Lederman D, Moran T J and Schuller I K 1996 *Phys. Rev. Lett.* **76** 4624
Moran T J, Nogues J, Lederman D and Schuller I K 1998 *Appl. Phys Lett.* **72** 617
Lederman D, Nogues J and Schuller I K 1997 *Phys. Rev.* B **56** 2332
Moran T J, Gallego J M and Schuller I K 1995 *J. Appl. Phys.* **78** 1887
Michel R P, Chaiken A, Wang C T and Johnson L E 1998 *Phys. Rev.* B **58** 8566
[11] Unguris J, Celotta R J and Pierce D T 1992 *Phys. Rev. Lett.* **69** 1125